RAPID COMMUNICATIONS

PHYSICAL REVIEW B VOLUME 44, NUMBER 11 15 SEPTEMBER 1991-I

Fe on Au(100): Quantum-well states down to a monolayer

F. J. Himpsel
IBM Research Division, Thomas J. Watson Research Center, P. O. Box 218, Yorktown Heights, New York 10598
(Received 17 June 1991)

Quantum-well states are observed for Fe films embedded in Au(100) using inverse photoemission. They can be analyzed with a simple interferometer model, using bulk states from the $\Gamma_{12}\Delta_1 H_{15}$ band that are modulated by an envelope function with wavelengths in the order of 7–10 atomic layers (10–14 Å). These states can be followed down to a monolayer, where two states are seen at 0.6 and 1.9 eV. They are tentatively assigned to the $\Delta_5\downarrow$ monolayer state and a Δ_1 quantum-well state. The resulting ferromagnetic exchange splitting of the Δ_5 state is 2.7 eV, exceeding the splitting of 1.8–2.1 eV for the analogous bulk band.

The attempts to fabricate ever finer quantum structures, such as superlattices and quantum wells, are approaching the atomic limit. The study presented here makes the connection from a narrow but still bulklike quantum well to a monolayer quantum well. The latter is strongly influenced by interface phenomena since the atoms in the well are all interface atoms. The transition from conventional quantum-well states to monolayer states is observed with inverse photoemission. In contrast to previously studied quantum wells, such as semiconductors and noble metals, the system considered here consists of a ferromagnetic well, all the way down to a monolayer. In the monolayer limit a ferromagnetic exchange splitting of 2.7 eV is found for the Δ_5 state, which is significantly larger than the splitting of 1.8–2.1 eV for the analogous bulk band. This confirms predictions of enhanced monolayer magnetism.

The Fe/Au(100) system is suited particularly well for the purpose of creating narrow quantum wells. There is a good lattice match (better than 1%), with the lattice constant of fcc Au a factor of $\sqrt{2}$ larger than that of bcc Fe. This provides a one-to-one match of the (100) surface lattices, due to the extra face-centered atom in Au. The two band structures, however, are quite different from each other, thereby providing a large band offset and well depth of 9 eV. This is an order of magnitude larger than in any other quantum-well system studied to date.[1–7] As a consequence, the exponential decay of the wave function is extremely fast in the barrier region, thereby confining the states to the well within a single layer. The growth of Fe on Au(100) has been found to proceed layer-by-layer,[8,9] with one layer of Au staying on top of the growing Fe surface.[8] This Au overlayer acts as a surfactant by lowering the surface energy of the growing film and thereby preventing island formation. The resulting uniformity of the Fe film makes it possible to see variations in the electronic structure on a layer-by-layer basis. Since Fe is capped on both sides by Au one obtains a nearly symmetric quantum-well structure.

The Au(100) substrate was electropolished (using a cyanide-based method), sputtered (500 eV Ar^+ at $\pm 30°$ from grazing), and annealed (400 °C). It exhibited a bright 5×20 low-energy electron-diffraction (LEED) pattern, which converted to 1×1 at submonolayer Fe coverage. Fe was evaporated from a miniature electron-beam evaporator with a rate of 7 Å/min at a pressure in the 10^{-10} Torr range. The Au substrate temperature was room temperature for the data shown. Deposition at elevated substrate temperature gave somewhat sharper inverse photoemission spectra and LEED spots, but the thickness was less reproducible due to Fe-Au interdiffusion. The film thickness was measured with a quartz-crystal monitor. As a cross-check, the energy of the image potential surface state (see Fig. 1) was found to decrease until the completion of the first layer, and then stayed constant. This image state energy, however, is still much closer to that of Au(100) than that of Fe(100), confirming that Au has segregated to the growing Fe(100) surface.

The development of overlayer states from the submonolayer range to the quantum-well regime is shown in Fig. 1. It is striking to see how rapidly the spectra change with Fe coverage. Peaks turn into valleys by just adding one or two layers, e.g., the peak at 2 eV when going from 1 to 2 layers, or the peak at 5 eV when going from 5 to 7 layers. This indirectly confirms that the quantum wells are homogeneous within one layer. In the following, we will first discuss the states in the 2–10-layer regime, which turn out to be traditional quantum-well states, produced by quantizing the momentum $k^{\perp}$ of bulk bands along the direction perpendicular to the interfaces. This approach is expected to fail when approaching the monolayer regime, where the Fe atoms experience the potential of Au neighbors instead of Fe. As characteristic cases, the monolayer quantum well and the dilute submonolayer limit will be discussed at the end, including their enhanced magnetic moments.

The simplest view of a quantum well is that of an interferometer, e.g., the Fabry-Perot geometry indicated as an inset of Fig. 2 (see also Ref. 10). Changing the thickness of the well is equivalent to changing the spacing between the two plates in the optical analog. Consequently, one expects interference maxima to repeat themselves when the round-trip path length after two reflections changes by the wavelength λ, corresponding to a change of the spacing by $\lambda/2$. Indeed, the intensity of the inverse-photoemission signal at a given energy exhibits oscillatory behavior with overlayer thickness (Fig. 2). From the period-

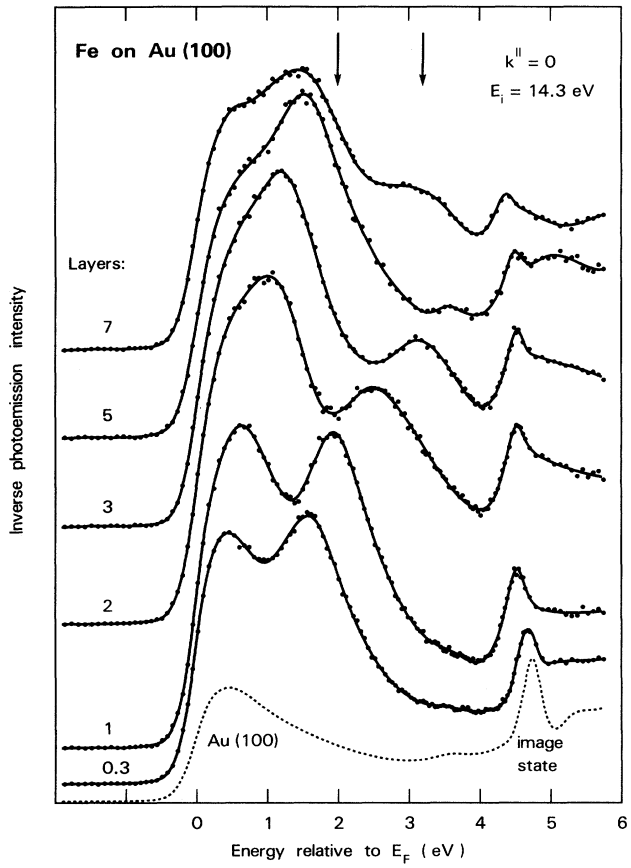

FIG. 1. Inverse-photoemission spectra at normal incidence for Fe layers on Au(100). Quantum-well states in the Fe layer show up as peaks that vary strongly with film thickness, e.g., in the 2–4 eV range. They are confined by Bragg reflection at the Au(100) substrate and at a segregated Au overlayer.

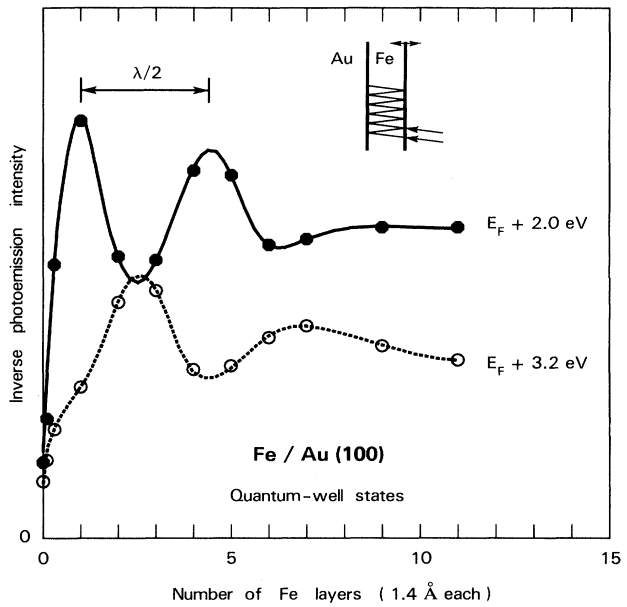

FIG. 2. Oscillations of the inverse-photoemission intensity with quantum-well thickness, measured at the two energies that are indicated by arrows in Fig. 1. The period of these oscillations corresponds to half the wavelength of a quantum-well state, like for the interference fringes of an optical interferometer (inset).

icity we can directly read off the wavelength λ, and the momentum $k^{\perp}=2\pi/\lambda$ of the quantum-well states. For example, at an energy of 2.0 eV above the Fermi level E_F one finds a period $p=3.4$ layers resulting in $\lambda=6.8$ layers $=9.5$ Å with a layer spacing $d=1.4$ Å, and $k^{\perp}=0.66$ Å$^{-1}=k^{ZB}/p$, where $k^{ZB}=\pi/d$ is the momentum at the boundary H of the bulk Brillouin zone in the [100] direction (see Fig. 3 and Refs. 11–13). Going up in energy, the oscillation period increases ($\lambda=9.5$, 11, 14 Å at 2.0, 3.2, 5.7 eV, respectively), and the phase of the oscillations changes. For example, the first maximum occurs at 0.3 times the period for an energy of 2.0 eV, corresponding to a phase of 0.6π. It increases to 1.3π at 3.2 eV and to 2π at 5.7 eV. The phase of the oscillations is determined by the phase shifts for reflection at the two Fe-Au boundaries. On the bulk Au(100) side we have a clear-cut Bragg reflection since the band structure exhibits a gap of states between the X_4' and X_1 points (Fig. 3). For Bragg reflection at such an "inverted" band gap the phase shift changes from 0 at the "antibonding" X_4' point to π at the "bonding" X_1 point. The detailed energy dependence of the phase shift can be calculated using a simple two-band model.[14] For example, one obtains phase shifts of 0.3, 0.5, 0.9π at 2.0, 3.2, 5.7 eV, respectively. This calculated phase shift at the substrate interface can be subtracted from the measured total phase shift to estimate the phase shift for the reflection at the Au overlayer. The resulting overlayer phase shifts are comparable to those of the substrate (e.g., 0.3, 0.8, 1.1π at 2.0, 3.2, 5.7 eV), showing that a monolayer of Au reflects already quite similar to bulk Au.

The momentum $k^{\perp}$ obtained from the intensity-versus-thickness oscillations represents the momentum of the so-called envelope function.[1] This envelope function modulates a rapidly oscillating Bloch wave function that is derived from band-edge states in the quantum well. In our case, the band edge of the Fe quantum well is formed by the H_{15} point at the Brillouin-zone boundary (Fig. 3). To obtain the total momentum one has to combine the momentum $k_0^{\perp}$ of the band-edge states with the momentum $\pm k^{\perp}$ of the envelope function. Plotting energy versus total momentum one obtains the data points in Fig. 3 (open circles). Considering the error bars from the uncertainty in thickness calibration ($\approx \pm 30\%$) the data generally follow the dispersion of the bulk Δ_1 band of Fe. There seems to be some deviation towards lower energies when going away from the zone boundary. This corresponds to thinner quantum wells (i.e., larger $k^{\perp}$), and may indicate a lowering of the potential by the Au atoms adjacent to the well. The best way to study this phenomenon is to go to the extreme, i.e., to a monolayer well.

For the monolayer case the band structure simplifies since all Fe atoms become equivalent. At $k^{\parallel}=0$ the Fe $3d$

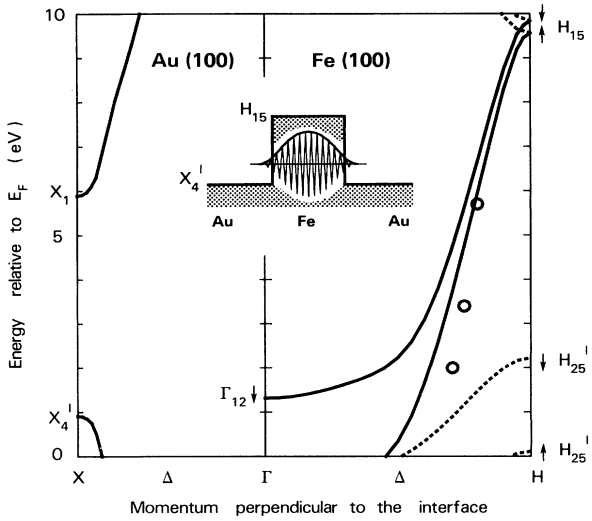

FIG. 3. Band diagram for a Fe-in-Au(100) quantum well along the [100] interface normal. Both Au(100) and Fe(100) exhibit band gaps of Δ_1 symmetry (X_4'-X_1 and H_{15}-H_{12} with H_{12} at 21 eV not shown, see Refs. 11–13). The lower band edges X_4' and H_{15} form a 9-eV deep, hole-type quantum well analogous to that for the valence band in semiconductors. Only bands with allowed transitions in normal incidence are shown, i.e., Δ_1 (solid) and Δ_5 (dashed). The open circles are derived from the quantum-well oscillations in Fig. 2.

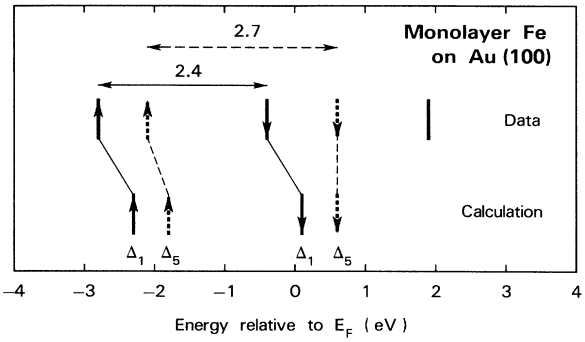

FIG. 4. Electronic states for a monolayer of Fe on Au(100). Photoemission (Ref. 17) and inverse-photoemission data are compared with a local-density calculation (Ref. 15) for states of Δ_1 and Δ_5 symmetry, which are the only ones reachable with normal emission/incidence electrons. The ferromagnetic exchange splitting of the Δ_5 state is larger than that of the analogous bulk band [2.7 eV vs 1.8–2.1 eV (Ref. 13)], indicating an enhanced magnetic moment in the monolayer.

manifold splits due to the fourfold C_{4v} symmetry into four states, i.e., $\Delta_1(d_{z^2})$, $\Delta_2(d_{x^2-y^2})$, $\Delta_2'(d_{xy})$, and the doubly degenerate $\Delta_5(d_{xz,yz})$. Only two of these are accessible for normal incidence (or emission) electrons, i.e., Δ_1 with the photon field **E** parallel to the interface and Δ_5 with **E** perpendicular. These states can be distilled from the complicated, published monolayer band structures[15,16] by their symmetry. The result for a monolayer of Fe on Au(100) is shown in Fig. 4 (bottom, extracted from Ref. 15), and compared to a spin-polarized photoemission study[17] and the inverse-photoemission results. The calculated states all have a counterpart in the data that is consistent with the reported[17] spin and symmetry. Thereby we tentatively assign the lower of the two inverse-photoemission peaks (at 0.6 eV) to the $\Delta_5\downarrow$ state, based on its connectivity with the bulk $\Delta_5\downarrow$-$H_{25}'\downarrow$ peak when going to thick Fe(100) films (compare Ref. 3 for bulk Fe). This assignment gives a ferromagnetic exchange splitting of 2.7 eV for the Δ_5 state, which is significantly larger than that of the corresponding bulk band (Γ_{25}'-Δ_5-H_{25}'), i.e., 2.1 eV for Γ_{25}' and 1.8 eV for H_{25}' (see Ref. 13). Using the empirical correlation of 1 eV/μ_{Bohr} found between the exchange splitting and the magnetic moment[18] one may conclude that the magnetic moment of the monolayer is enhanced compared to that of the bulk. This is in line with predictions[15,16] of enhanced monolayer magnetism. It should be noted, however, that the splitting of 2.4 eV reported[17] for the occupied Δ_1 monolayer state is equal to the splitting of the corresponding bulk band (Γ_{12}-Δ_1, see Ref. 13).

The Δ_1 states of the monolayer in Fig. 4 are pulled down by more than 1 eV below the bottom of the corresponding bulk bands (i.e., Γ_{12}-Δ_1, see Fig. 3 and Ref. 13). This must be the influence of the Au neighbors at the interface. The same trend was already noticeable for the thinner quantum wells, where the quantum-well states plotted in Fig. 3 lie below the Δ_1 bulk bands. This shows the limitations of a simple, bulklike quantum-well model when approaching wells in the monolayer range. In addition to the *d*-like states discussed so far there exists an extra inverse-photoemission peak at 1.9 eV for the embedded monolayer. It connects with the quantum-well states at higher coverage, which also have Δ_1 symmetry (Fig. 3). This peak has some *s*,*p* character, judging from the energy dependence of its cross section. Relative to the *d*-like $\Delta_5\downarrow$ peak at 0.6 eV its intensity increases at lower electron energy (not shown). Thus there are two candidates for the extension of the quantum-well states to a monolayer.

Below monolayer coverage the ferromagnetic, long-range order disappears. The Curie temperature has been found to drop below room temperature somewhere between 0.5 and 1 layer.[19,20] The inverse-photoemission peaks shift downwards from their monolayer positions (0.6 and 1.9 eV) to ≤ 0.25 and 1.5 eV in the limit of zero coverage. This shift is too small to account for a collapse of the ferromagnetic splitting (see Fig. 4). It is likely that there exists a local magnetic moment that causes a magnetic splitting. The situation is probably close to the spin-glass phase[21] formed by dilute Fe in Au. In this case a large, local moment of $3.7\mu_{\text{Bohr}}$ has been found, even larger than the moment of $2.97\mu_{\text{Bohr}}$ predicted[15] for the monolayer and close to the atomic limit of $4\mu_{\text{Bohr}}$. Photoemission from the spin-glass phase[21] has identified a Fe 3*d* peak near the Fermi level as the partially filled minority spin state. This would be consistent with the inverse-photoemission peak at ≤ 0.25 eV being the empty part of this state. A similarity between submonolayer film and dilute spin glass has already been noticed[22] for Mn on Ag versus Mn in Ag. A two-dimensional version of the spin-glass phase may be the ultimate fate of magnetic layers in the low coverage limit, where long-range ferromagnetic order ceases to exist but local moments are still present, or

even increasing.

The results on quantum-well states can be summarized as follows: Quantum-well states give rise to intensity-versus-thickness oscillations in inverse photoemission, which are related to the wavelength of the envelope function. The wavelength ranges from 10 to 14 Å, which is suspiciously close to the period of an oscillatory exchange coupling observed recently in magnetic superlattices[23] (typically 7–18 Å). Whether or not there is a connection remains to be explored. The quantum-well states can be traced all the way down to the submonolayer regime, where their energy is lowered by interface bonding.

[1]G. Bastard, *Wave Mechanics Applied to Semiconductor Heterostructures* (Les Editions de Physique, Les Ulis, France, 1988), in particular, see Chap. III.

[2]R. E. Thomas, J. Appl. Phys. **41**, 5330 (1970); R. C. Jaklevic and John Lambe, Phys. Rev. B **12**, 4146 (1975).

[3]Hiroshi Iwasaki, B. T. Jonker, and Robert L. Park, Phys. Rev. B **32**, 643 (1985).

[4]S. Å. Lindgren and L. Walldén, Phys. Rev. Lett. **61**, 2894 (1988).

[5]T. Miller, A. Samsavar, G. E. Franklin, and T.-C. Chiang, Phys. Rev. Lett. **61**, 1404 (1988); M. A. Mueller, A. Samsavar, T. Miller, and T.-C. Chiang, Phys. Rev. B **40**, 5845 (1989); M. A. Mueller, T. Miller, and T.-C. Chiang, *ibid.* **41**, 5214 (1990).

[6]N. B. Brookes, Y. Chang, and P. D. Johnson, Phys. Rev. Lett. **67**, 354 (1991).

[7]P. D. Loly and J. B. Pendry, J. Phys. C **16**, 423 (1983).

[8]S. D. Bader and E. R. Moog, J. Appl. Phys. **61**, 3729 (1987).

[9]R. Germar, W. Dürr, J. W. Krewer, D. Pescia, and W. Gudat, Appl. Phys. A **47**, 393 (1988).

[10]R. S. Becker, J. A. Golovchenko, and B. S. Swartzentruber, Phys. Rev. Lett. **55**, 987 (1985); G. Binnig, K. H. Frank, H. Fuchs, N. Garcia, B. Reihl, H. Rohrer, F. Salvan, and A. R. Williams, Phys. Rev. Lett. **55**, 991 (1985).

[11]R. Lässer, N. V. Smith, and R. L. Benbow, Phys. Rev. B **24**, 1895 (1981).

[12]J. Callaway and C. W. Wang, Phys. Rev. B **16**, 2095 (1977); J. Callaway (private communication).

[13]A. Santoni and F. J. Himpsel, Phys. Rev. B **43**, 1305 (1991).

[14]A.-W. Maue, Z. Phys. **94**, 717 (1935); N. V. Smith, Phys. Rev. B **32**, 3549 (1985); P. M. Echenique and J. B. Pendry, Prog. Surf. Sci. **32**, 111 (1990).

[15]C. L. Fu, A. J. Freeman, and T. Oguchi, Phys. Rev. Lett. **54**, 2700 (1985); Chun Li, A. J. Freeman, and C. L. Fu, J. Magn. Magn. Mater. **75**, 201 (1988); Chun Li, A. J. Freeman, H. J. F. Jansen, and C. L. Fu, Phys. Rev. B **42**, 5433 (1990).

[16]Roy Richter, J. G. Gay, and John R. Smith, Phys. Rev. Lett. **54**, 2704 (1985).

[17]W. Heinen, C. Carbone, T. Kachel, and W. Gudat, J. Electron Spectrosc. Relat. Phenom. **51**, 701 (1990).

[18]F. J. Himpsel (unpublished).

[19]S. D. Bader, E. R. Moog, and P. Grünberg, J. Magn. Magn. Mater. **53**, L295 (1986).

[20]W. Dürr, M. Taborelli, O. Paul, R. Germar, W. Gudat, D. Pescia, and M. Landolt, Phys. Rev. Lett. **62**, 206 (1989).

[21]H. S. Reehal and P. T. Andrews, J. Phys. F **10**, 1631 (1980).

[22]W. Drube and F. J. Himpsel, Phys. Rev. B **35**, 4131 (1987).

[23]S. S. P. Parkin, N. More, and K. P. Roche, Phys. Rev. Lett. **64**, 2304 (1990); S. S. P. Parkin, R. Bhadra, and K. P. Roche, *ibid.* **66**, 2152 (1991); A. Cebollada, R. Miranda, C. M. Schneider, P. Schuster, and J. Kirschner (unpublished).